ARTICLE

NAPE-PLD in the ventral tegmental area regulates reward events, feeding and energy homeostasis

Julien Castel[1], Guangping Li[1], Oriane Onimus[1], Emma Leishman[2], Patrice D. Cani[3,4,5], Heather Bradshaw[2], Ken Mackie[2,6], Amandine Everard[1,3,4,5], Serge Luquet[1,8]✉ and Giuseppe Gangarossa[1,7,8]✉

The *N*-acyl phosphatidylethanolamine-specific phospholipase D (NAPE-PLD) catalyzes the production of *N*-acylethanolamines (NAEs), a family of endogenous bioactive lipids, which are involved in various biological processes ranging from neuronal functions to energy homeostasis and feeding behaviors. Reward-dependent behaviors depend on dopamine (DA) transmission between the ventral tegmental area (VTA) and the nucleus accumbens (NAc), which conveys reward-values and scales reinforced behaviors. However, whether and how NAPE-PLD may contribute to the regulation of feeding and reward-dependent behaviors has not yet been investigated. This biological question is of paramount importance since NAEs are altered in obesity and metabolic disorders. Here, we show that transcriptomic meta-analysis highlights a potential role for NAPE-PLD within the VTA→NAc circuit. Using brain-specific invalidation approaches, we report that the integrity of NAPE-PLD is required for the proper homeostasis of NAEs within the midbrain VTA and it affects food-reward behaviors. Moreover, region-specific knock-down of NAPE-PLD in the VTA enhanced food-reward seeking and reinforced behaviors, which were associated with increased in vivo DA release dynamics in response to both food- and non-food-related rewards together with heightened tropism towards food consumption. Furthermore, midbrain knock-down of NAPE-PLD, which increased energy expenditure and adapted nutrient partitioning, elicited a relative protection against high-fat diet-mediated body fat gain and obesity-associated metabolic features. In conclusion, these findings reveal a new key role of VTA NAPE-PLD in shaping DA-dependent events, feeding behaviors and energy homeostasis, thus providing new insights on the regulation of body metabolism.

Molecular Psychiatry; https://doi.org/10.1038/s41380-024-02427-6

INTRODUCTION

The regulation of feeding behaviors and energy homeostasis is a cardinal and evolutionarily conserved physiological feature in mammals. By mobilizing several and functionally distinct brain circuits [1, 2], such regulation tightly depends on metabolic and nutritional demands as well as on the reinforcing and hedonic properties of foods. Among the different regulatory pathways which signal homeostatic states and scale feeding behaviors, lipids, either nutritional and/or endogenous species, represent key mediators in gating the functional adaptability of complex neuronal networks that synchronize food intake and energy expenditure [3, 4].

Endogenous bioactive lipids are a major class of biologically active mediators which critically regulate several functions, spanning from homeostasis to cognition. Among these, the membrane phospholipids-derived long-chain fatty acids *N*-acylethanolamines (NAEs) are potent signaling molecules in peripheral tissues as well as in the central nervous system (CNS). Given their wide distribution and multiple biological functions, the modulation of NAEs tone represents an interesting target for the development of new therapeutic approaches [5].

Among NAEs, the *N*-arachidonoylethanolamine (AEA or anandamide), a bona fide endocannabinoid (eCB) agonist of the cannabinoid receptors CB1R and CB2R, is synthetized by the Ca^{2+}-dependent enzyme *N*-acyl phosphatidylethanolamine-specific phospholipase D (NAPE-PLD) [6, 7] from the membrane *N*-acylphosphatidylethanolamine (NAPE). However, the enzyme NAPE-PLD is also important for the synthesis of other NAEs that do not bind to CBRs, including *N*-oleoylethanolamine (OEA), *N*-palmitoylethanolamine (PEA) and *N*-stearoylethanolamine (SEA) [5]. In fact, while AEA binds to the cannabinoid receptors CB1R, CB2R and the transient receptor potential vanilloid 1 (TRPV1) [8], OEA, PEA and SEA activate several non-cannabinoid receptors, including peroxisome proliferator-activated receptors (PPARα), GPR55 and GPR119 [9, 10]. Importantly, these NAEs are involved in the regulation of appetite and energy homeostasis through different mechanisms [11–15], notably by acting within the gastrointestinal tract [13, 16], at the gut-brain interface

[1]Université Paris Cité, CNRS, Unité de Biologie Fonctionnelle et Adaptative, F-75013 Paris, France. [2]Department of Psychological and Brain Sciences, Indiana University Bloomington, Bloomington, IN, USA. [3]Metabolism and Nutrition Research group, Louvain Drug Research Institute (LDRI), UCLouvain, Université catholique de Louvain, Brussels, Belgium. [4]WELBIO-Walloon Excellence in Life Sciences and Biotechnology, WELBIO department, WEL Research Institute, Wavre, Belgium. [5]Institute of Experimental and Clinical Research (IREC), UCLouvain, Université catholique de Louvain, Brussels, Belgium. [6]Gill Center for Biomolecular Science, Indiana University Bloomington, Bloomington, IN, USA. [7]Institut universitaire de France (IUF), Paris, France. [8]These authors contributed equally: Serge Luquet, Giuseppe Gangarossa. ✉email: serge.luquet@u-paris.fr; giuseppe.gangarossa@u-paris.fr

Received: 24 July 2023 Revised: 7 January 2024 Accepted: 9 January 2024

[9, 17, 18] and/or directly in the brain [19–21]. While NAPE-PLD expression, enzymatic activity and related byproducts have been detected in the mouse, rat and human brains [7, 22–24], the key functions of this enzyme within the brain remain elusive and not well-elucidated. In fact, most of the current literature has focused on distinct NAEs based on their transducing effectors (receptors, transcription factors) and not on the enzyme itself. Only recently, a few studies have shown that pharmacological blockade of NAPE-PLD activity [25] or selective ablation of NAPE-PLD in stress-activated neurons [21] impaired limbic functions (fear extinction, anxiety) mainly through the regulation of the hypothalamus-pituitary-adrenal (HPA) axis, thus highlighting the importance of NAPE-PLD and its NAEs in brain functions. Furthermore, NAPE-PLD silencing and consequent increased availability of its NAPE substrate are neuroprotective in response to 6-OHDA-induced loss of dopamine (DA)-neurons [20], suggesting an important role of NAPE-PLD in regulating physiological and cellular functions of DA-neurons.

Moreover, the developmental invalidation of the Napepld gene alters very-long chain fatty acids composition in the brain, suggesting a more complex role for NAPE-PLD than previously appreciated and the existence of alternative biosynthetic pathways [26, 27]. Furthermore, the non-CB1R-related signaling engaged by fatty acid ethanolamines (FAEs) produced by the specific enzymatic activity encoded by the Napepld gene (ID: 242864) points toward a role for this enzyme in the generation of bioactive FAEs with a wide array of functions including the regulation of energy balance (OEA), inflammation (PEA) or pain sensitivity (SEA).

Interestingly, the presence of a single-nucleotide polymorphism (SNP) on the coding region of the Napepld gene (rs17605251) has been associated with severe obesity (BMI ≥ 35 kg/m^2) [28, 29], suggesting a potential role for NAPE-PLD in the regulation of energy homeostasis, food-motivated behaviors and metabolic disorders.

In the present study, we took advantage of several integrative in vivo approaches following genetic and/or viral induction of tissues-specific deletion of NAPE-PLD in basal, food-motivated and obese conditions. Within the mouse mesolimbic reward system, notably the ventral tegmental area (VTA), we found that the enzyme NAPE-PLD functions as a fine-tuning gatekeeper of reward events and DA dynamics as well as an important regulator of energy homeostasis and metabolic efficiency in both physiological and pathological (obesity) contexts.

MATERIALS AND METHODS

Animals

All experimental procedures were approved by the Animal Care Committee of the Université Paris Cité (CEB-06-2017, APAFiS #11033) and carried out following the 2010/63/EU directive. Details are provided as Supplemental Information.

Drugs

GBR12909 (10 mg/kg, Tocris), cocaine hydrochloride (15 mg/kg, Sigma-Aldrich) and tamoxifen (10 mg/ml, 100 µl/day, MP Biomedicals) were used. Details are provided as Supplemental Information.

Viral constructs

pAAV-hsyn-GRAB_DA2m was a gift from Yulong Li (Addgene plasmid #140553; http://n2t.net/addgene:140553; RRID:Addgene_140553).

pAAV.CMV.HI.eGFP-Cre.WPRE.SV40 was a gift from James M. Wilson (Addgene plasmid #105545; http://n2t.net/addgene:105545; RRID:Addgene_105545).

pAAV.CMV.PI.eGFP.WPRE.bGH was a gift from James M. Wilson (Addgene plasmid #105530; http://n2t.net/addgene:105530; RRID:Addgene_105530)

Stereotaxic surgery

Anesthetized mice (see Supplemental Information for details) were placed on a stereotactic frame (David Kopf Instruments, California, USA). Bilateral (AAV-GFP or AAV-Cre-GFP in the VTA, 0.2 µl/side) or unilateral (GRAB-DA2m in the NAc, 0.3 µl) micro-injections were performed at the following coordinates (in mm from bregma): VTA (L = +/−0.45; AP = −3.4, V = −4.3) and NAc (L = −0.9; AP = +1.18, V = −4.4).

In vivo fiber photometry

For in vivo dopamine imaging (GRAB-DA2m [30]), a chronically implantable cannula (Doric Lenses, Québec, Canada), composed of a bare optical fiber (400 µm core, 0.48 N.A.) and a fiber ferrule, was implanted 100 µm above the viral injection site (NAc). Real time fluorescence was recorded as previously described [31, 32]. Details are provided as Supplemental Information.

Metabolic efficiency analysis

Metabolic efficiency was measured as previously described [31]. Briefly, mice were monitored for whole energy expenditure (EE), O_2 consumption, CO_2 production, respiratory exchange ratio (RER = VCO_2/VO_2, V = volume), and locomotor activity using calorimetric cages (Labmaster, TSE Systems GmbH, Bad Homburg, Germany). Details are provided as Supplemental Information.

Animal behaviors

All behavioral paradigms and procedures are provided as Supplemental Information.

Tissue preparation and immunofluorescence

Anaesthetized mice were transcardially perfused with cold PFA 4% for 5 min. Sections were processed and confocal imaging acquisitions were performed as previously described [32, 33]. Primary antibodies used: rabbit anti-TH (1:1000, Merck Millipore, #AB152) and rabbit anti-cFos (1:500, Synaptic Systems, #226003). Quantifications were performed using the cell counter plugin of ImageJ taking a fixed threshold of fluorescence as standard reference.

Lipidomics

Tissue extracts and HPLC/MS/MS were performed as previously described [34]. Details are provided as Supplemental Information.

Reclustering and transcriptomics meta-analysis

Publicly available transcriptomic data were downloaded from Gene Expression Omnibus (GSE137763, GSE168156, GSE64526, GSE114918) and analyzed using R pipelines generated in line with the original publications. See also Supplemental Information.

Statistics

All data are presented as mean ± SEM. Statistical tests were performed with Prism 7 (GraphPad Software, La Jolla, CA, USA). Detailed statistical analyses are listed in the Supplementary Table 1. Normality was assessed by the D'Agostino-Pearson test. Data were analyzed using either Student's *t* test (paired or unpaired) with equal variances, one-way or two-way ANOVA. The significance threshold was automatically set at $p < 0.05$. ANOVA analyses were followed by Bonferroni post hoc test for specific comparisons.

RESULTS

NAPE-PLD is functionally expressed in the brain and mediates motivational food-responses

We first addressed the consequence of whole-body NAPE-PLD developmental knock-out in a food-reward seeking behavioral paradigm. Here, we used the Napepld$^{f/f}$ mouse line in which the two LoxP sites span the exon 3 [18, 24, 35, 36]. Napepld$^{f/f}$ mice were bred with mice expressing Cre under the pan-promoter phosphoglycerate kinase 1 (Pgk-Cre) which result in whole-body full knock-out (KO [37]) of NAPE-PLD in subsequent generations. To study the reinforcing and motivational properties of food, we performed an operant conditioning paradigm where animals were trained, under different schedules, to press a lever to obtain a palatable sugar pellet. In both a fixed ratio 1 schedule (FR1, 1 lever press for 1 sugar pellet during 4 daily sessions) or a progressive ratio schedule (PR), which assesses the motivational component of

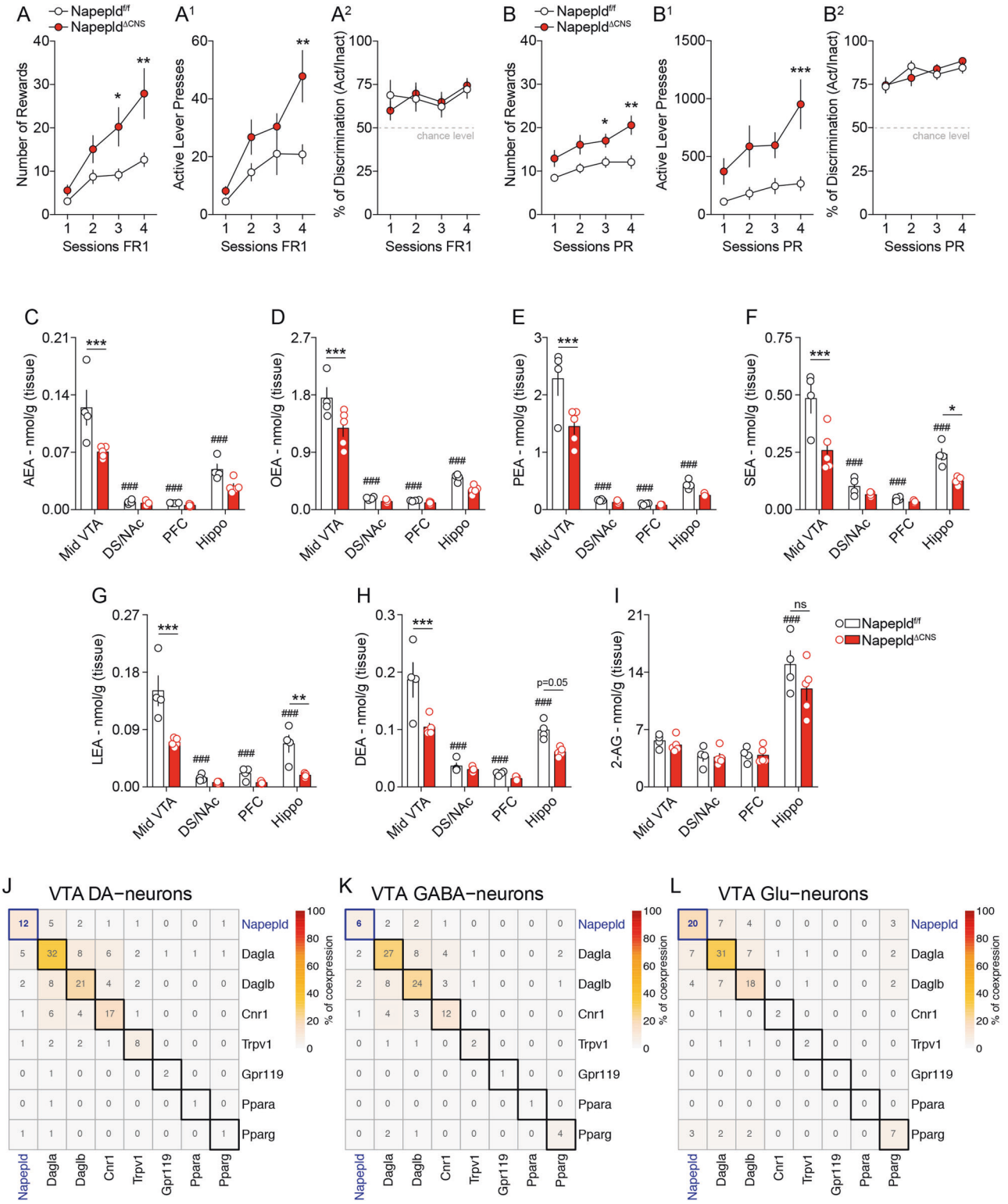

reinforced behaviors, Napepld$^{+/+}$ (controls) and Napepld^{KO} mice displayed similar performances (Supplementary Fig. 1A, B). These results suggest that either physiological compensations occurred during development, as reported by previous genetic invalidations [27], and/or that, despite the expression of NAPE-PLD in the brain [23], brain NAPE-PLD plays a marginal role in reward-seeking behavior. To disentangle these two hypotheses, we moved to brain-restricted ablation of NAPE-PLD by crossing Napepld$^{f/f}$ mice with Nestin-Cre mice (Nes$^{Cre+/-}$ mice) [38, 39]. Genetic deletion of NAPE-PLD in the central nervous system (CNS) was associated with an enhanced response to operant behavior characterized by a higher number of pellets and active lever presses under a FR1 schedule (Fig. 1A, A^1, both males and females), while discrimination scores (% of active lever over inactive lever) were similar between genotypes (Fig.1A^2). Despite similar learning scores, Napepld$^{\Delta CNS}$ mice showed enhanced performances

Fig. 1 Deletion of NAPE-PLD in the nervous system promotes reward seeking behaviors and reduces *N*-acylethanolamines in the VTA. The reward-seeking phenotype of Napepld$^{f/f}$ and Napepld$^{\Delta CNS}$ mice was tested through an operant conditioning paradigm (lever press). **A**-A^2 Operant conditioning during 4 consecutive sessions with a fixed ratio 1 (FR1) schedule. **A** Number of rewards, (A^1) number of active lever presses and (A^2) percentage of discrimination between the active and inactive lever presses. **B**-B^2 Operant conditioning during 4 consecutive sessions with a progressive ratio (PR) schedule. **B** Number of rewards, (B^1) number of active lever presses and (B^2) percentage of discrimination between the active and inactive lever presses. **C**–**H** Lipidomic analysis of *N*-acylethanolamines (NAEs) and **I** 2-AG in the midbrain ventral tegmental area (VTA), the dorsal striatum/nucleus accumbens (DS/NAc), the prefrontal cortex (PFC) and the hippocampus (Hippo) of Napepld$^{f/f}$ and Napepld$^{\Delta CNS}$ mice. Anandamide (AEA), *N*-oleoylethanolamine (OEA), *N*-palmitoylethanolamine (PEA), *N*-stearoylethanolamine (SEA), *N*-linoleoylethanolamine (LEA), *N*-docosahexaenoylethanolamine (DEA), 2-Arachidonoylglycerol (2-AG). **J**–**L** Meta-analysis and clustering of snRNA-seq results in the rat VTA focusing on NAEs- and endocannabinoids (eCBs)-related synthesis machineries and receptors. Percentage (%) of co-expression of *Napepld* in the VTA dopamine (DA)-neurons (**J**, 379 neurons), VTA GABA-neurons (**K**, 1741 neurons) and VTA glutamate (Glu)-neurons (**L**, 662 neurons) (extracted from [46]). Statistics: $^*p < 0.05$, $^{**}p < 0.01$ and $^{***}p < 0.001$ for Napepld$^{\Delta CNS}$ *vs* Napepld$^{f/f}$ mice; $^{\#\#\#}p < 0.001$ for VTA *vs* other brain structures (Napepld$^{f/f}$ mice). For number of mice/group and statistical details see Supplementary Table 1.

(number of rewards and active lever presses) compared to control mice under a PR schedule (Fig. 1B, B^1, B^2). To exclude that such phenotype was driven by the presence of Cre (Nes$^{Cre+/-}$ [38, 40]) rather than the proper deletion of NAPE-PLD, we performed the same behavioral battery in Nes$^{Cre-/-}$ (controls) and Nes$^{Cre+/-}$ mice which both displayed a very similar phenotype on this paradigm (Supplementary Fig. 1C, D), thus indicating that genetic deletion of neuronal NAPE-PLD is responsible for the enhanced reward-behavior observed in Napepld$^{\Delta CNS}$ mice. This finding, which points to an effective role of brain NAPE-PLD in food-reward seeking behaviors, also raises the possibility that the contribution of NAPE-PLD in multiple organs (full KO mice) might lead to physiological adjustments eventually driving opposite consequences on a particular behavioral output with an overall mitigated consequence.

Among the main organs that might contribute to food-dependent reward processes, the gut has emerged as a critical modulator of reinforced behaviors [3, 31, 41, 42]. It has been previously shown that mice with a specific and inducible deletion of NAPE-PLD in the intestinal epithelial cells (IEC) (Napepld$^{\Delta IEC}$) exhibited a phenotype associated with specific changes in the homeostatic regulation of food intake and altered metabolic adaptations to high-fat diet [18, 43]. Therefore, we explored the potential contribution of intestinal NAPE-PLD in reward-seeking behavior. Interestingly, Napepld$^{\Delta IEC}$ and control mice showed comparable performances in the operant conditioning paradigm (Supplementary Fig. 1E, F), indicating that, while intestinal NAPE-PLD is critical for metabolic control [18] and short-term regulation of food intake [43], brain NAPE-PLD might represent a more direct target as regulator of food-reward behaviors.

Reinforced behaviors tightly depend on key brain regions that constitute the reward system, notably the midbrain dopamine (DA)-producing ventral tegmental area (VTA) and its dopaminoceptive structures, including the dorsal striatum (DS)/nucleus accumbens (NAc), the prefrontal cortex (PFC) and the hippocampus (Hippo) [44]. Therefore, we first investigated whether NAPE-PLD-produced NAEs were altered within these structures in Napepld$^{\Delta CNS}$ mice. Lipidomic analyses revealed a significant decrease of several NAEs species [AEA, OEA, PEA, *N*-stearoylethanolamine (SEA), *N*-linoleoylethanolamine (LEA) and *N*-docosahexaenoylethanolamine (DEA)] in the midbrain VTA following CNS deletion of NAPE-PLD (Fig. 1C–H). Interestingly, either no major differences (DS/NAc and PFC), specific significant reductions (SEA, LEA and DEA for the hippocampus) or trends of decrease were detected in the levels of NAEs in the other reward-associated brain regions (Fig. 1C–H). Of note, no alterations were detected for the endocannabinoid (eCB) 2-AG (Fig. 1I). Moreover, within the VTA we did not detect alterations in the levels of other fatty acids (linoleic, arachidonic and oleic acids) (Supplementary Fig. 2A–C) or N-acylamides (Supplementary Table 2), thus indicating that lack of NAPE-PLD specifically affects a subset of endogenous bioactive lipids.

In addition, lipidomic analyses also revealed that NAEs, but not 2-AG (Fig. 1I), levels were higher in the VTA compared to the DS/NAc, PFC and hippocampus (Fig. 1C–H).

These biochemical results, associated to the enhanced reward-seeking phenotype of Napepld$^{\Delta CNS}$ mice (Fig. 1A, B), prompted us to investigate the structure- and/or cell type-specific expression of NAPE-PLD in both rodents (rat and mouse) and human brains. First, by taking advantage of single-nucleus RNA transcriptomics (snRNA-seq) in the rat NAc [45] (GSE137763) and VTA [46] (GSE168156), we performed clustering meta-analyses of transcripts encoding for eCBs- and NAEs-producing enzymes (*Napepld*, *Dagla*, *Daglb*) as well as for eCBs- and NAEs-related transducing effectors (*Cnr1*, *Trpv1*, *Gpr119*, *Ppara*, *Pparg*). Compared to *Dagla* and *Daglb*, we observed that accumbal *Drd1*- and *Drd2*-medium spiny neurons (MSNs) expressed low levels of *Napepld* (6% of *Drd1*-MSNs and 5% of *Drd2*-MSNs, respectively) (Supplementary Fig. 3A, B). In the VTA, we again detected higher levels of *Dagla* and *Daglb* but, interestingly, we observed that *Napepld* was mainly present in VTA DA- and Glu-neurons [12% of DA-neurons (Fig. 1J) and 20% of Glu-neurons (Fig. 1L), respectively], whereas 6% of GABA-neurons were positive for *Napepld* (Fig. 1K). Of note, less than 10% of VTA mixed-neurons co-expressed *Napepld* (Supplementary Fig. 3C, D). Interestingly, the pattern of *Napepld* expression mirrored the higher levels of NAEs observed in the VTA compared to the DS/NAc (Fig. 1C). Moreover, the transcriptomic profiling of eCBs- and NAEs-producing enzymes was in line with the meta-analysis of bulk VTA transcriptomics in the murine [47] (*Slc6a3*-bacTRAP mice, GSE64526, Supplementary Fig. 3E) and human midbrains [48] (GSE114918, Supplementary Fig. 3F).

Altogether these observations underline the potential role for NAPE-PLD in the midbrain VTA as a regulator of food-associated reward processes.

VTA NAPE-PLD scales food-motivated behaviors and dopamine releasing dynamics

Next, we knocked-down the Napepld gene in the VTA using a local and virally mediated delivery of Cre in the VTA of Napepld$^{f/f}$ mice (Napepld$^{VTA-GFP}$ and Napepld$^{\Delta VTA}$ mice, Fig. 2A). Expression of Cre-GFP was observed in both TH-positive (31.6%, 286 out of 906 cells) and TH-negative cells (Fig. 2B) and led to a basal activation (cFos expression, Fig. 2C) in the VTA of Napepld$^{\Delta VTA}$ compared to control Napepld$^{VTA-GFP}$ mice (Fig. 2C^1). Although, cFos was mainly increased in Cre-GFP$^+$-cells (as compared to control GFP$^+$-cells, Fig. 2C^2), we observed a slight but significant increase also in Cre-GFP$^-$-cells (Fig. 2C^3), indicating that disruption of NAEs synthesis in a subset of VTA-neurons may also influence the activity of neighbor neurons (local communication).

In line with the results obtained with Napepld$^{\Delta CNS}$ mice (Fig. 1A, B), we observed that viral deletion of NAPE-PLD in the VTA promoted food-operant conditioning (increased number of rewards and active lever presses) during both FR1 and PR schedules (Fig. 2D, E), with no differences in learning performances (Fig. 2D, E). This enhanced

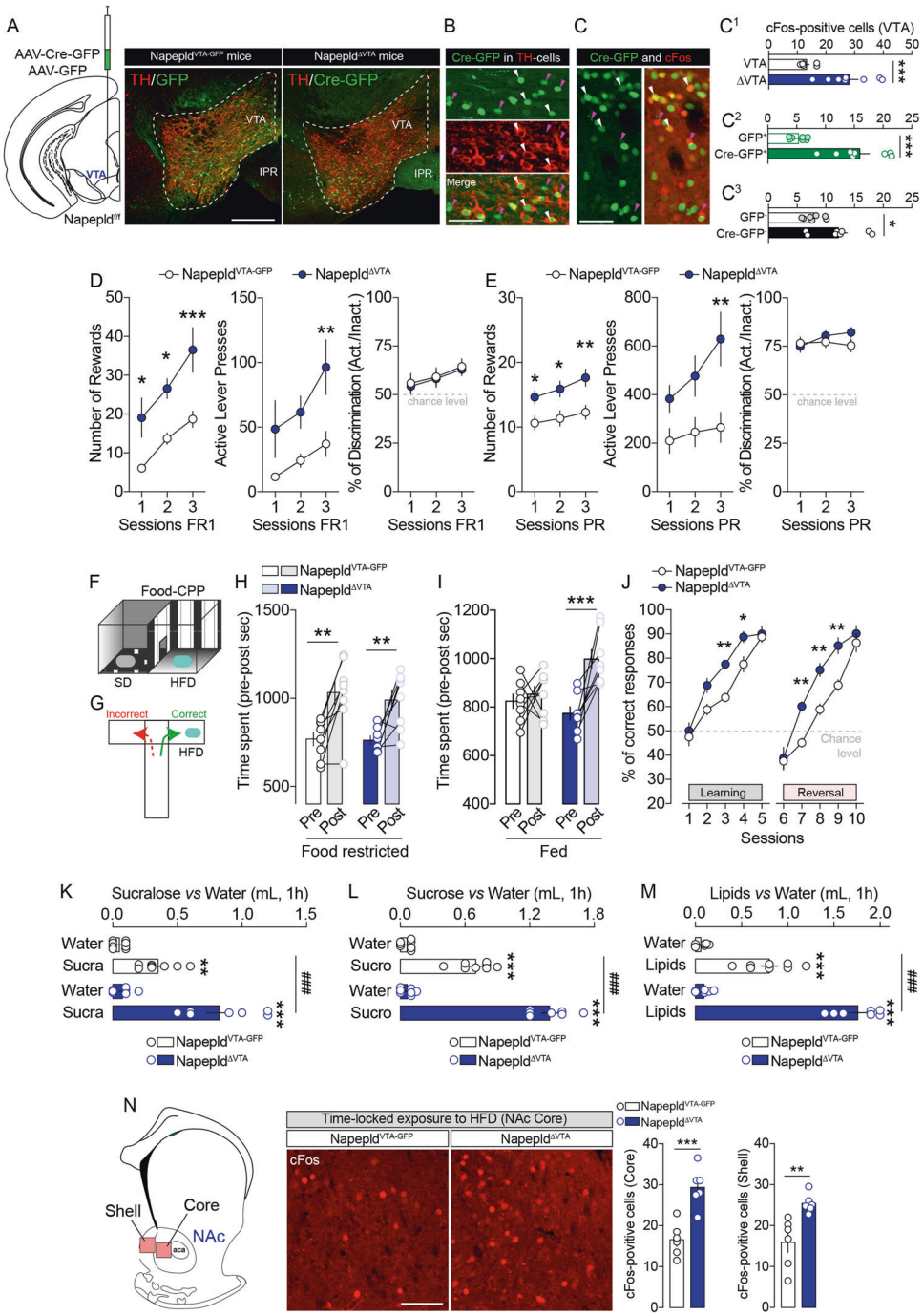

reward-seeking phenotype was also present following a FR1→FR5→PR training schedule (Supplementary Fig. 4A–C, food restriction and Supplementary Fig. 4D, sated conditions), in both males and females (Supplementary Fig. 4E–H), with no significant differences in initial body weight and body weight loss (food restriction) between experimental groups (Supplementary Fig. 5A, B). These results exclude the potentially confounding effect of hunger onto motivational drive.

Aside from the motivational component, the liking and learning components of feeding are an integral part of food-reward processes [44]. These components can be assessed through behavioral measurements of the positive valence assigned to palatable food in the conditioned-place preference (CPP, Fig. 2F) and T-maze (Fig. 2G) paradigms, which rely on the association between reward value and context. In food-restricted conditions, we observed an increased and similar CPP score in both Npepld$^{VTA\text{-}GFP}$ and Npepld$^{\Delta VTA}$ mice (Fig. 2H). However, in sated conditions, only Npepld$^{\Delta VTA}$ mice showed an HFD-induced increase in CPP score (Fig. 2I), indicating enhanced susceptibility to the reinforcing properties of palatable foods. Using the T-maze paradigm, we assessed the ability and flexibility of mice to actively learn in discriminating between a rewarded (HFD) and a non-rewarded arm. During the learning phase (first 5 days), both groups showed a progressive increase in correct responses (%) over training days, with Npepld$^{\Delta VTA}$ mice performing significantly better than control mice (Fig. 2J). Then, mice were tested for their flexibility to relearn the task under a reversal learning schedule (in which the food reinforcer was switched to the previously

Fig. 2 NAPE-PLD knock-down in the VTA promotes reward-seeking behaviors and food preference. A Scheme and immunofluorescence sections indicating the viral injection of AAV-Cre-GFP or AAV-GFP in the VTA of Napepld$^{f/f}$ mice. Scale bar: 250 µm. **B** Expression of Cre-GFP in TH-positive and TH-negative cells. White arrows indicate co-localization, magenta arrows indicate no co-localization. Scale bar: 50 µm. **C** Expression of cFos in Cre-GFP^{+}- and Cre-GFP^{-}-cells. White arrows indicate co-localization, magenta arrows indicate no co-localization. Scale bar: 50 µm. (C^{1-3}) Quantifications and comparisons of cFos-positive cells within the VTA between Napepld$^{VTA\text{-}GFP}$ and Napepld$^{\Delta VTA}$ mice (C^1), GFP^{+}- and Cre-GFP^{+}-cells (C^2), GFP^{-}- and Cre-GFP^{-}-cells (C^3). Operant conditioning during 3 consecutive sessions with a FR1 (**D**) and a PR (**E**) schedule. For both schedules the number of rewards, the number of lever presses and the percentage of discrimination between the active and inactive lever presses are shown. **F**, **G** Drawings indicate the food-induced conditioned-place preference (CPP) and the T-Maze paradigms, respectively. **H** CPP in Napepld$^{VTA\text{-}GFP}$ and Napepld$^{\Delta VTA}$ food-restricted mice (10% of body weight reduction). **I** CPP in Napepld$^{VTA\text{-}GFP}$ and Napepld$^{\Delta VTA}$ sated mice. **J** Learning and reversal learning performances of Napepld$^{VTA\text{-}GFP}$ and Napepld$^{\Delta VTA}$ food-restricted mice (10% of body weight reduction) in the T-Maze. Food preference in Napepld$^{VTA\text{-}GFP}$ and Napepld$^{\Delta VTA}$ mice using three different choices: sucralose *vs* water (**K**), sucrose *vs* water (**L**), and lipids *vs* water (**M**). **N** Detection and quantification of cFos-positive cells in the NAc of Napepld$^{VTA\text{-}GFP}$ and Napepld$^{\Delta VTA}$ mice following the exposure to a fixed amount of high-fat diet (HFD). Scale bar: 100 µm. Statistics: $^{*}p < 0.05$ and $^{***}p < 0.001$ for Napepld$^{\Delta VTA}$ *vs* Napepld$^{VTA\text{-}GFP}$ mice (C^1), Cre-GFP^{+}- *vs* GFP^{+}-cells (C^2), Cre-GFP^{-} *vs* GFP^{-}-cells (C^3). Statistics: $^{*}p < 0.05$, $^{**}p < 0.01$ and $^{***}p < 0.001$ for Napepld$^{\Delta VTA}$ *vs* Napepld$^{VTA\text{-}GFP}$ mice (**D**, **E**, **J**, **N**). Statistics: $^{**}p < 0.01$ and $^{***}p < 0.001$ for Napepld$^{\Delta VTA}$ (post- *vs* pre-test in CPP) or Napepld$^{VTA\text{-}GFP}$ (post- *vs* pre-test in CPP) (**H**, **I**). Statistics: $^{**}p < 0.01$ and $^{***}p < 0.001$ for Napepld$^{\Delta VTA}$ (sucra/sucro/lipids *vs* water) or Napepld$^{VTA\text{-}GFP}$ mice (sucra/sucro/lipids *vs* water) (**K**, **L**, **M**); $^{\#\#\#}p < 0.001$ for Napepld$^{\Delta VTA}$ *vs* Napepld$^{VTA\text{-}GFP}$ mice (**K**, **L**, **M**). For number of mice/group and statistical details see Supplementary Table 1.

unreinforced arm of the T-maze). While both groups displayed good performance in learning/flexibility, VTA-specific deletion of NAPE-PLD resulted in a better performance with a more rapid acquisition of the correct entry into the reinforced arm as compared to Napepld$^{VTA\text{-}GFP}$ control mice (Fig. 2J).

Next, we investigated the role of VTA NAPE-PLD in driving palatable food preference during a time-locked window (1 h of exposure). First, we tested the reinforcing properties of the non-caloric sweetener sucralose (2 mM). As shown in Fig. 2K, Napepld$^{\Delta VTA}$ mice consumed more sucralose than Napepld$^{VTA\text{-}GFP}$ control mice. A very similar pattern was measured with the natural caloric sugar sucrose (10%, Fig. 2L) and with emulsified lipids (20%, Fig. 2M).

We therefore decided to investigate whether the enhanced reward-like phenotype observed in Napepld$^{\Delta VTA}$ mice was associated to an increased activity of the nucleus accumbens (NAc), a region highly innervated by VTA projections and whose activity is correlated with food-reward processes [44]. However, the enhanced neural response within the reward system might result either from the higher tropism/consumption of palatable food of Napepld$^{\Delta VTA}$ mice or from the increased rewarding value despite a fixed amount of food-reinforcer. In order to dissociate these two possibilities, we exposed our experimental groups (sated conditions) to an equal amount of HFD during a time-locked window (1 h during which all mice consumed the HFD pellet) and then we analyzed the induction of cFos in the NAc (Fig. 2N). Interestingly, we detected more cFos-positive cells in both NAc Core and Shell subregions of Napepld$^{\Delta VTA}$ mice (Fig. 2N), indicating an enhanced responsiveness of the VTA→NAc mesolimbic axis.

These results led us to hypothesize that VTA NAPE-PLD and its local NAEs bioproducts may contribute to the regulation of DA dynamics within the VTA→NAc mesolimbic axis. To test this hypothesis, we took advantage of in vivo fiber photometry coupled to virally expressed DA biosensors (GRAB-DA2m [30]) to measure DA dynamics in the NAc of Napepld$^{VTA\text{-}GFP}$ and Napepld$^{\Delta VTA}$ mice (Fig. 3A, B). First, we observed that exposing both fasted and *ad libitum* fed mice to HFD triggered a higher DA accumulation/release in the NAc of Napepld$^{\Delta VTA}$ mice compared to control animals (Fig. 3C–E, and Supplementary Fig. 6A).

Second, to further explore whether NAPE-PLD contributes to the regulation of DA-dependent events, we tested in vivo DA dynamics also in two non-food-dependent paradigms: the administration of cocaine (Fig. 3G, H) and the tail suspension (TS, Fig. 3I, J and Supplementary Fig. 6B). In both cases, we observed that Napepld$^{\Delta VTA}$ mice were characterized by an enhanced accumulation/release of DA in the NAc as compared to Napepld$^{VTA\text{-}GFP}$ mice. Lastly, we administered the selective DAT blocker GBR12909 and noticed an enhanced locomotor response in Napepld$^{\Delta VTA}$ mice (Supplementary Fig. 6C), further confirming an amplified DA release/tone as a consequence of VTA NAPE-PLD knock-down.

Overall, these results indicate that VTA NAPE-PLD tightly contributes in orchestrating the responses of DA-neurons to both food- and non-food-related reinforcers by promoting and boosting the release of DA at VTA→NAc synapses.

VTA NAPE-PLD contributes to the regulation of food intake and energy homeostasis

New evidence indicates that the reward system also strongly contributes in scaling whole-body metabolic functions [49, 50]. We therefore explored the metabolic consequences of knocking-down VTA NAPE-PLD in the regulation of whole-body metabolic efficiency and peripheral substrates utilization by using longitudinal measurements of indirect calorimetry. As previously observed (Supplementary Fig. 5), no major differences were observed in body weight and body composition between the two experimental groups (Fig. 4A). However, Napepld$^{\Delta VTA}$ mice displayed a spontaneous increase in locomotor activity and in food intake compared to Napepld$^{VTA\text{-}GFP}$ mice during both the light and dark circadian phases (Fig. 4B, B^1, C, C^1). These phenotypes were associated with an overall enhanced energy expenditure (Fig. 4D, D^1) and to a change in peripheral substrates utilization favoring carbohydrates- over lipids-based substrates as indicated by the increased respiratory exchange ratio (RER, 1=glucose substrate, 0.7=lipids substrate) during the light phase (Fig. 4E, E^1) and the consequent decrease in fatty acid oxidation (FAO) in Napepld$^{\Delta VTA}$ mice during both the light and dark phases (Fig. 4F, F^1). This feature was also associated with enhanced glucose tolerance during an oral glucose tolerance test at the expense of lower insulin release, suggesting enhanced whole-body glucose dynamics and insulin sensitivity (Supplementary Fig. 7).

We then decided to investigate how Napepld$^{\Delta VTA}$ mice adapted during manipulation of nutrient availability. We noticed that during a food deprivation period (overnight fasting) Napepld$^{\Delta VTA}$ mice were still characterized by increased locomotor activity (Fig. 4G) and energy expenditure (Fig. 4I), with no differences in RER (Fig. 4J). While the capability to mobilize lipids-based substrates during the fasting-induced lipolysis was similar between the two groups, as indicated by the RER (Fig. 4J), the proportion of lipids used as primary source of fuel was enhanced during the fasting period (FAO, Fig. 4K), indicating a metabolic shift toward lipids-based substrates utilization. Interestingly, upon refeeding, mice displayed no significant differences in food intake (Fig. 4H), locomotor activity (Fig. 4G) or substrates utilization

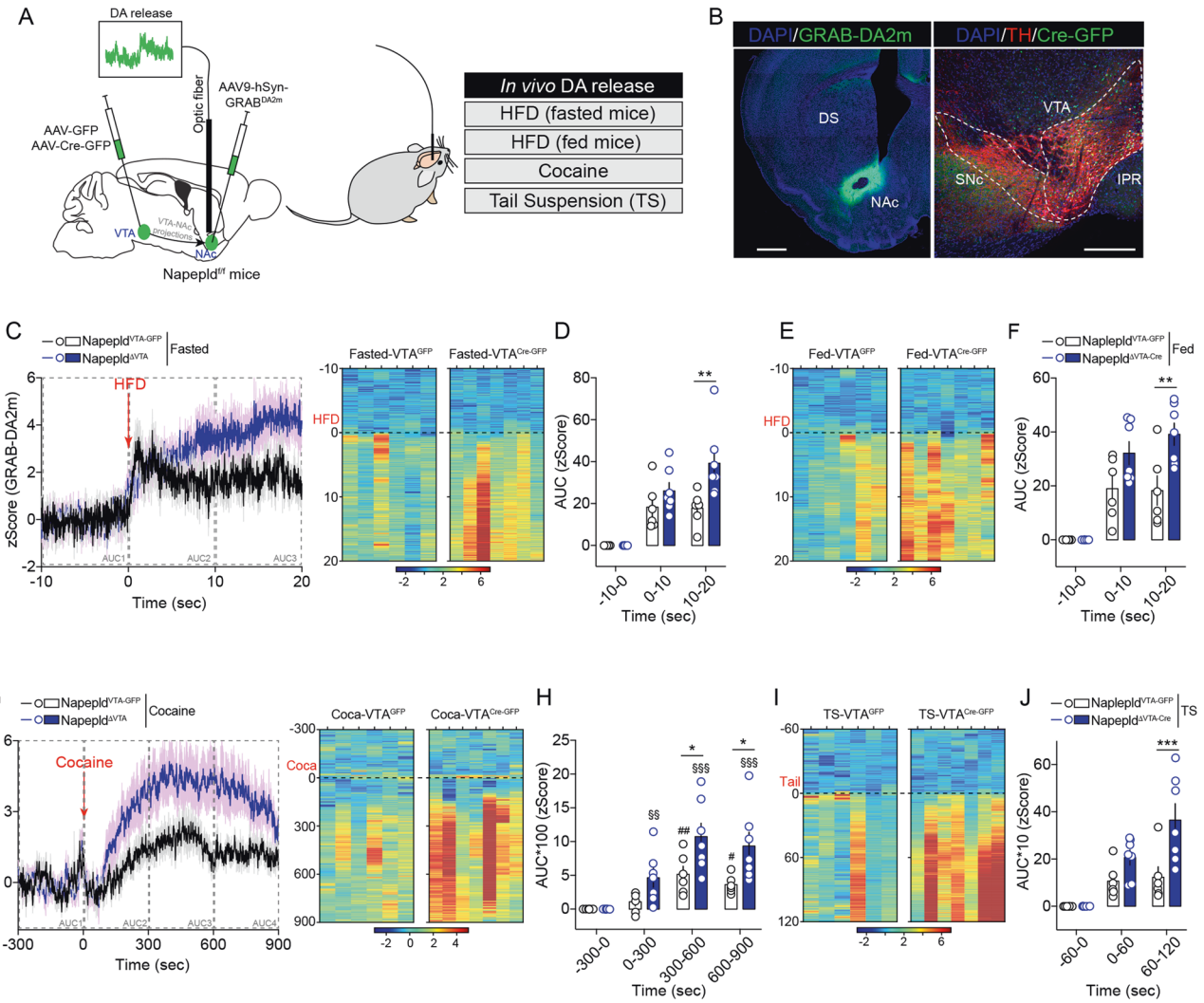

Fig. 3 NAPE-PLD knock-down in the VTA regulates in vivo DA release dynamics. A Drawing indicates the double viral strategies to record in vivo DA dynamics in Napepld$^{VTA\text{-}GFP}$ and Napepld$^{\Delta VTA}$ mice by using fiber photometry coupled to the DA biosensor GRAB-DA2m. DA dynamics were measured during food- and non-food-dependent behaviors. **B** Immunofluorescence detection of GRAB-DA2m in the NAc and AAV-Cre-GFP in the VTA (with TH staining). Scale bars: 250 µm. Temporal dynamics and/or heatmaps of DA releasing dynamics in Napepld$^{VTA\text{-}GFP}$ and Napepld$^{\Delta VTA}$ mice during consumption of HFD in both fasted (**C**, **D**) and fed (**E**, **F**) conditions as well as during cocaine administration (**G**, **H**) and tail suspension (**I**, **J**). Statistics: $^{*}p < 0.05$, $^{**}p < 0.01$ and $^{***}p < 0.001$ for Napepld$^{\Delta VTA}$ *vs* Napepld$^{VTA\text{-}GFP}$ mice; $^{\#}p < 0.05$ and $^{\#\#}p < 0.01$ for cocaine time course in Napepld$^{VTA\text{-}GFP}$ mice; $^{\S\S}p < 0.01$ and $^{\S\S\S}p < 0.01$ for cocaine time course in Napepld$^{\Delta VTA}$ mice. For number of mice/group and statistical details see Supplementary Table 1.

(Fig. 4J, K), while a slight increase in energy expenditure was still detected in Napepld$^{\Delta VTA}$ mice (Fig. 4I). These results confirmed the hypothesis that the integrity of NAPE-PLD within the VTA was required for the proper metabolic adaptation to changes in nutrient availability.

Since fasting increases the motivational drive and responsiveness to food, we wondered whether the expression of NAPE-PLD was required to promote DA releasing dynamics in fasted mice exposed to a chow pellet. In contrast to the acute response to palatable HFD (Fig. 3C–F), consumption of a chow pellet resulted in similar DA releasing dynamics in both Napepld$^{VTA\text{-}GFP}$ and Napepld$^{\Delta VTA}$ mice (Fig. 4L, M). This may suggest that (*i*) the action of VTA NAPE-PLD in the modulation of adaptive metabolic responses to nutritional manipulations can be dissociated from DA release in the fast-refeeding transition and/or (*ii*) VTA NAPE-PLD plays an active role in discriminating between palatable (HFD, Fig. 3C–F) and regular (chow, Fig. 4L, M) foods through the control of reward-dependent DA dynamics.

VTA NAPE-PLD does not contribute to exercise-motivated behaviors but still regulates energy homeostasis

In mammals, exercise can function as a rewarding/motivational stimulus [51] and the eCBs system, especially within the VTA, has been identified as a key regulator of exercise-induced reinforced behaviors [52–54]. We thus decided to extend our investigations to exercise-motivated behaviors (*i*) to investigate whether VTA NAPE-PLD was also important in mediating the reinforcing properties of exercise and (*ii*) to study whether metabolic adaptations observed in Napepld$^{\Delta VTA}$ mice (Fig. 4) were solely dependent on enhanced locomotor activity.

First, we performed a time-locked access (30 min session/day) to a running wheel. Despite both Napepld$^{VTA\text{-}GFP}$ and Napepld$^{\Delta VTA}$ mice progressively spent more time wheel-running, we surprisingly noticed a reduced performance in Napepld$^{\Delta VTA}$ mice compared to control animals (Fig. 5A, A[1]). This led us to investigate whole-body metabolism and metabolic efficiency in calorimetric chambers equipped with running wheels.

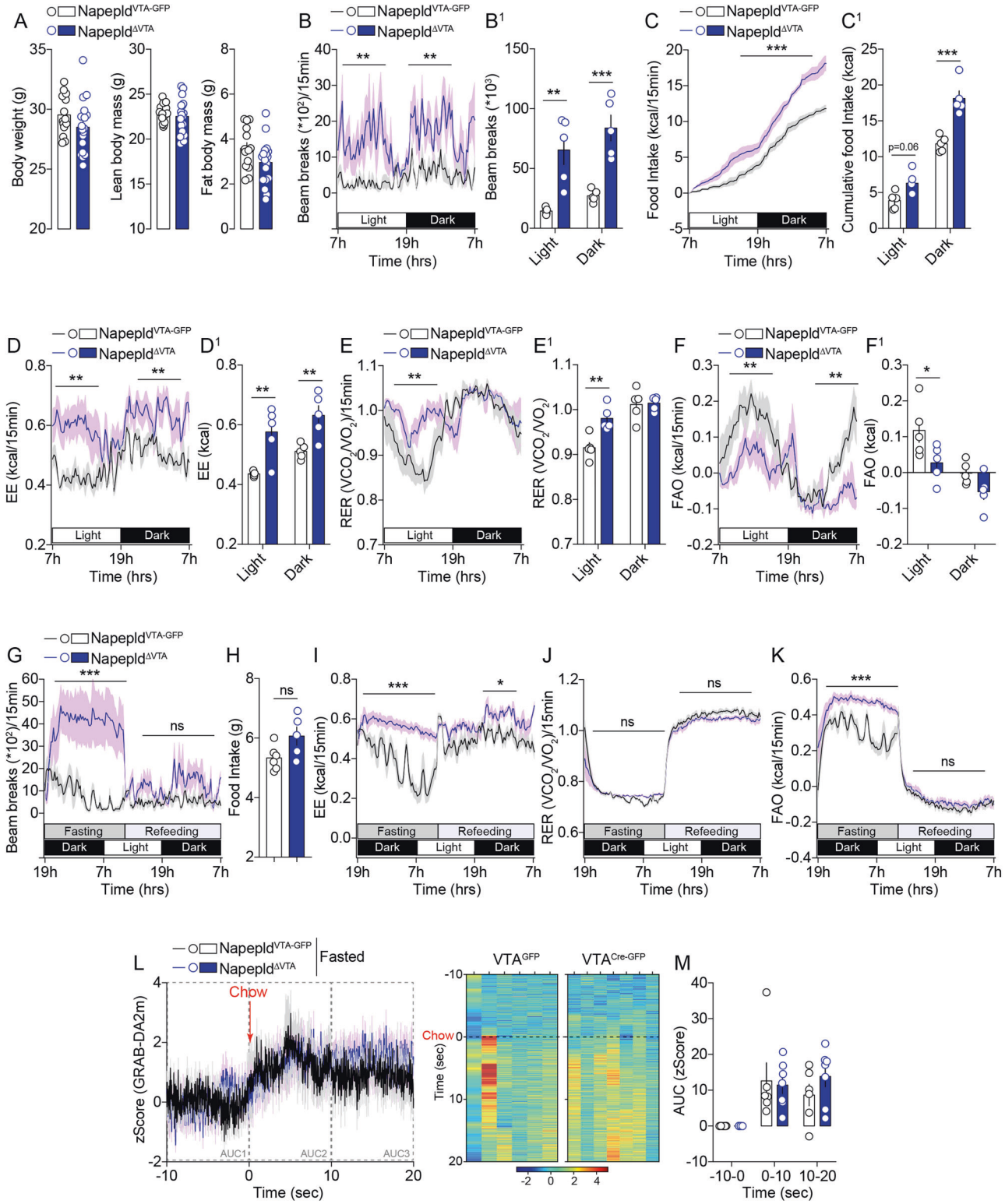

Fig. 4 VTA NAPE-PLD contributes to the regulation of energy balance and metabolic efficiency. A Body weight and body composition of Napepld$^{VTA\text{-}GFP}$ and Napepld$^{\Delta VTA}$ mice. **B**–**K** Indirect calorimetric studies in Napepld$^{VTA\text{-}GFP}$ and Napepld$^{\Delta VTA}$ mice to assess energy balance and metabolic efficiency. Longitudinal measurements in calorimetric chambers of locomotor activity (**B**, B^1), food intake (**C**, C^1), energy expenditure EE (**D**, D^1), respiratory exchange ratio RER (**E**, E^1) and fatty acid oxidation FAO (**F**, F^1) in Napepld$^{VTA\text{-}GFP}$ and Napepld$^{\Delta VTA}$ sated mice. **G**–**K** Indirect calorimetric studies in Napepld$^{VTA\text{-}GFP}$ and Napepld$^{\Delta VTA}$ mice undergoing a fasting/refeeding metabolic challenge. **G** Locomotor activity, **H** cumulative food intake, **I** energy expenditure, **J** respiratory exchange ratio and **K** fatty acid oxidation. **L**, **M** Temporal kinetics and heatmaps of in vivo DA releasing dynamics in Napepld$^{VTA\text{-}GFP}$ and Napepld$^{\Delta VTA}$ fasted mice and exposed to a chow pellet. Statistics: $^*p < 0.05$, $^{**}p < 0.01$ and $^{***}p < 0.001$ for Napepld$^{\Delta VTA}$ *vs* Napepld$^{VTA\text{-}GFP}$ mice. For number of mice/group and statistical details see Supplementary Table 1.

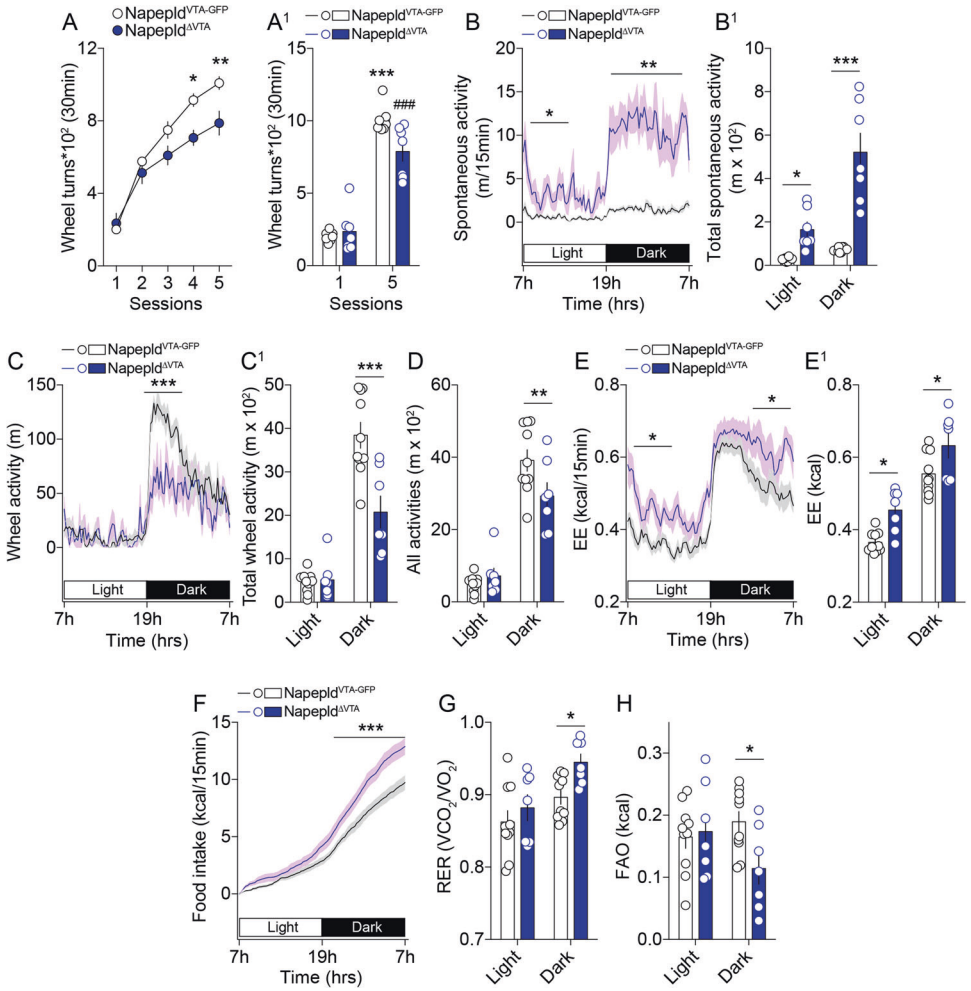

Fig. 5 VTA NAPE-PLD regulates energy balance independently from exercise. A, A[1] Time-locked (30 min/session) access to running wheels to mimic the reinforcing properties of exercise. **B**–**H** Indirect calorimetric studies in calorimetric chambers equipped with running wheels to assess energy balance and metabolic efficiency in Napepld$^{VTA\text{-}GFP}$ and Napepld$^{\Delta VTA}$ mice. **B**, B[1] Spontaneous locomotor activity, (**C**, C[1]) running wheel activity, (**D**) total locomotor activity (spontaneous + running wheel activities), (**E**, E[1]) energy expenditure, (**F**) cumulative food intake, (**G**) respiratory exchange ratio and **H** fatty acid oxidation. Statistics: *$p < 0.05$, **$p < 0.01$ and ***$p < 0.001$ for Napepld$^{\Delta VTA}$ *vs* Napepld$^{VTA\text{-}GFP}$ mice. For number of mice/group and statistical details see Supplementary Table 1.

Again, we observed that Napepld$^{\Delta VTA}$ mice were characterized by an enhanced spontaneous locomotor activity (Fig. 5B, B[1]) and reduced wheel-running activity (Fig. 5C, C[1]). When combining both forms of activity (spontaneous + wheel running activities), we detected no differences in the light phase and a lower global activity in Napepld$^{\Delta VTA}$ mice during the dark phase (Fig. 5D). Of interest, the peculiar metabolic signature associated with VTA NAPE-PLD deletion also remained in this exercise-based paradigm and was characterized by enhanced energy expenditure (Fig. 5E, E[1]), food intake (Fig. 5F) and RER (Fig. 5G), and lower FAO (Fig. 5H).

Altogether, these results indicate that the role of VTA NAPE-PLD in regulating reward-like processes cannot be generalized to all natural rewards (food *vs* exercise) and that the metabolic adaptations observed in VTA NAPE-PLD-deleted mice are not solely dependent on locomotor activity.

VTA NAPE-PLD controls metabolic adaptation to an obesogenic environment

Given the above-mentioned results, we hypothesized that NAPE-PLD may influence the (mal)adaptive responses to an obesogenic environment. Thus, Napepld$^{VTA\text{-}GFP}$ and Napepld$^{\Delta VTA}$ mice were chronically exposed to an obesogenic diet (3 months of HFD) and then metabolically characterized. First, we noticed no significant differences in the body weight and lean mass composition of both HFD-exposed experimental groups (Fig. 6A). However, fat body mass was significantly lower in Napepld$^{\Delta VTA}$ mice (Fig. 6A). The analysis of metabolic efficiency revealed that obese Napepld$^{\Delta VTA}$ mice displayed increased nocturnal locomotor activity (Fig. 6B) and enhanced nocturnal food intake (Fig. 6C, C[1]). Surprisingly, we detected a higher energy expenditure (Fig. 6D, D[1]) and FAO (Fig. 6E, E[1]) in obese Napepld$^{\Delta VTA}$ mice, whereas the RER resulted unchanged (Fig. 6F). This metabolic blueprint suggests that, depending on diets (chow *vs* HFD) and metabolic profiles (lean *vs* obese), VTA NAPE-PLD readily allows the plastic adaptation of nutrient partitioning (Fig. 4E, F *vs* Fig. 6E, F) in order to maintain a higher energy expenditure.

These results indicate that, within the VTA, the deletion of NAPE-PLD partially protects against diet-induced obesity.

DISCUSSION

It is now clear that NAPE-PLD bioproducts include important lipid mediators which, by acting on a variety of transcriptional and signaling cascades, control cellular and physiological responses [5]. In the present study we explored the role of NAPE-PLD in food- and reward-driven behaviors. Whole-body deletion of NAPE-PLD

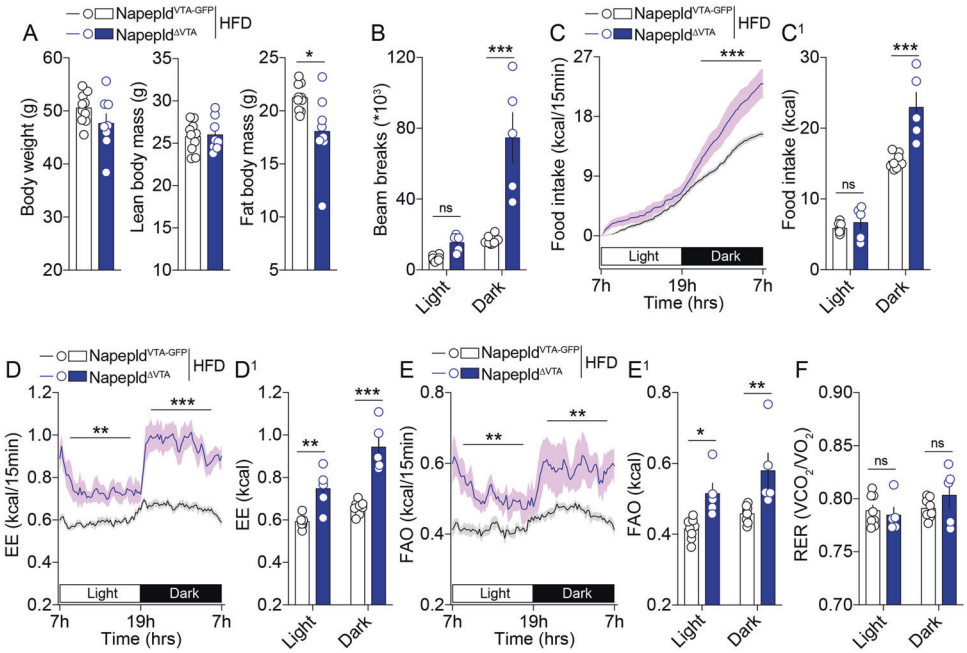

Fig. 6 VTA NAPE-PLD protects from obesity-associated metabolic features. A Body weight and body composition (fat and lean mass) of Napepld$^{VTA\text{-}GFP}$ and Napepld$^{\Delta VTA}$ mice exposed to chronic high-fat diet (HFD) and consequently characterized for energy balance and metabolic efficiency. **B** Cumulative locomotor activity, (**C**, C^1) food intake, (**D**, D^1) energy expenditure, (**E**, E^1) fatty acid oxidation and **F** respiratory exchange ratio. Statistics: *$p < 0.05$, **$p < 0.01$ and ***$p < 0.001$ for Napepld$^{\Delta VTA}$ *vs* Napepld$^{VTA\text{-}GFP}$ mice. For number of mice/group and statistical details see Supplementary Table 1.

did not affect food-reward operant conditioning, suggesting that compensatory mechanisms, as previously reported with a model of developmental NAPE-PLD KO mice [27], may be at play. However, using neural-specific genetic deletion (Nestin-Cre) or midbrain-specific viral invalidation approaches, we revealed that the integrity of NAPE-PLD within the midbrain VTA is required for NAEs synthesis (AEA, OEA, PEA, SEA, LEA and DEA) and that NAPE-PLD acts as a gatekeeper for fine-tuning food-reward behaviors and for regulating, at least as a contributor, energy balance and whole-body metabolism. In fact, viral down-regulation of NAPE-PLD in the VTA was associated with an enhanced tropism towards palatable foods, and stronger food reward-seeking and conditioning behaviors. Importantly, these behavioral adaptations were observed in both males and females, highlighting a well-conserved role of VTA NAPE-PLD. These phenotypes were associated, at least in part, with enhanced DA releasing dynamics in response to food rewards and also non-food-related stimuli. Consistent with the notion of a region-specific biosynthesis and action of NAEs, RNA-seq meta-analyses revealed low levels of *Napepld* in postsynaptic striatal dopaminoceptive neurons (NAc *Drd1*- and *Drd2*-MSNs), but a higher expression of *Napepld* in VTA-neurons, notably DA- and glutamate-neurons.

Previous studies focusing on nicotine reinforcement and tobacco use disorder (TUD) have shown that pharmacological inhibition of the fatty acid amide hydrolase (FAAH), one of the main enzymes responsible for the degradation of NAEs, reduces nicotine-enhanced DA transmission and nicotine reinforcement [19, 55] through the activation of PPARα by OEA/PEA and the activation of intracellular cascades, leading to the reduction of nicotinic receptors onto midbrain DA-neurons [19, 55]. In line with our results showing increased dopaminergic VTA→DA transmission following downregulation of VTA NAPE-PLD, these electrophysiological studies have clearly demonstrated that OEA/PEA inhibit DA-neurons, whereas inhibition of PPARα promotes their spontaneous activity [19, 56, 57]. However, these aforementioned seminal reports did not formally test nor establish the role of midbrain NAPE-PLD in these processes. In our hands, specific knock-down of NAPE-PLD in the VTA enhanced DA transmission in response to reward stimuli. In that view, our results are perfectly in line with a putative role for NAPE-PLD-derived substrates as negative modulators of VTA DA-neurons. At the ligand-receptor level, the negative control exerted by endogenous NAEs over the activity of VTA-neurons may be mediated by the variety of membrane and nuclear receptors (CB1R, TRPV1, PPARα, PPARγ) which scale the functions of VTA-neurons [19, 56–58]. Reduced production of NAEs (Napepld$^{\Delta CNS}$ and Napepld$^{\Delta VTA}$ in our study) may therefore alter this endogenous negative control leading to enhanced excitability of VTA-neurons through a disinhibitory process. In turn, this disinhibitory process may tune the activity of downstream VTA-projecting accumbal neurons which are involved in hedonic eating [59]. Indeed, the NAEs-associated receptor-specific driving forces of this regulatory control will need to be further investigated.

Our study, besides providing an additional mechanism by identifying NAPE-PLD as a potential candidate, also extends the role of this enzyme to the control of DA-dependent behaviors and DA releasing dynamics in response to reward-like stimuli. Although our results do not rule out whether the NAPE-PLD/NAPE→NAEs machinery controls both tonic and phasic DA release [60–62], they clearly indicate that VTA NAPE-PLD activity is an integral component of the control of DA-neurons responsiveness. Whether the cellular accumulation of NAPE and/or the decreased levels of NAEs are the primary responsible for the changes in DA-dependent behaviors and DA releasing dynamics is still unknown. Indeed, NAPE-PLD silencing seems to confer a protective action for increased NAPE species in 6-OHDA-induced neural damage [20], suggesting that the regulation of DA-neurons might be linked to NAPE/NAE membrane homeostasis. Given the multiple roles of endogenous bioactive lipids, it is possible that the invalidation of NAPE-PLD in the VTA may lead to an imbalance in the NAPE/NAEs ratio with ultimate consequences on a variety of processes including heightened DA responses to reward stimuli (i.e. disinhibition). In addition, NAEs, either cannabinoid-like (AEA) and non-cannabinoid-like (OEA, PEA) molecules, may be released

and act through several *modus operandi*. In fact, while the eCB AEA is retrogradely released *on demand* [63], the non-eCB NAEs may act anterogradely as suggested by the presence of NAPE-PLD also in pre-synaptic terminals [64], thus potentially modulating both intra-VTA microcircuits and/or VTA-projecting circuits (i.e. VTA→-NAc). However, the VTA does not only harbor DA-neurons [65, 66]. The relatively high expression of *Napepld* in VTA Glu-neurons may also indicate a possible regulatory control (i.e. inhibition by endogenous NAEs and disinhibition following NAPE-PLD deletion) of this cell type by the NAPE/NAEs ratio in the observed behavioral and metabolic features. This regulation may be exerted either through the local communication among the different neuronal VTA cell-types or through direct VTA^{Glu}→NAc projections. In fact, these glutamatergic projections, which can also convey rewarding effects [67, 68], were recently shown to promote reinforcement even independently of DA release [69]. Thus, we cannot exclude that NAPE-PLD-dependent mechanisms onto these complex neural networks may result from this additional form of VTA→NAc communication in encoding changes in reward-driven behaviors and metabolic efficiency. Despite this limitation, our in vivo imaging results clearly reveal that the VTA→NAc dopaminergic transmission is regulated, directly and/or indirectly, by NAPE-PLD. Indeed, further studies are warranted to fully flush out how and to which extent midbrain NAPE-PLD regulates DA events by selectively focusing on the local interconnectivity and interdependency of VTA DA-, Glu- and GABA-neurons.

Our study also unveils a key role of VTA NAPE-PLD in the control of whole-body metabolism and energy balance. At the circuit level, it is reasonable to speculate that an imbalanced activity of the VTA→NAc axis may in turn elicit adaptive changes within NAc-projecting hypothalamic structures, notably the lateral hypothalamus [70, 71], therefore leading to metabolic adaptations. NAPE-$PLD^{\Delta VTA}$ mice displayed increased spontaneous locomotor activity in both the fed and fasting, but not refed, conditions, which is consistent with an enhanced activity of VTA DA-neurons [72]. These features were associated with increased cumulative food intake and whole-body energy expenditure and, together with other recent studies [50, 73, 74], they point to the VTA as an important regulator of energy balance and metabolic efficiency. In fact, on chow diet the overall body weight was only marginally affected in NAPE-$PLD^{\Delta VTA}$ compared to control mice, suggesting that increased energy expenditure (EE) was compensated by increased energy intake in a closed and well-balanced homeostatic regulation (Fig. 5). During food deprivation, NAPE-$PLD^{\Delta VTA}$ mice showed a drastic increase in fasting-induced foraging, pointing towards a change in adaptive strategy in response to decreased nutrient availability. This increased activity was associated with increased EE and is most likely fueled by enhanced lipid-based metabolism (Fig. 5). In mice exposed to HFD, a similar increase in spontaneous activity, EE and FAO was observed together with increased food intake. Since NAPE-$PLD^{\Delta VTA}$ mice show increased tropism and responsiveness to palatable foods it is possible that overeating may be the result of enhanced palatability for energy-dense foods. An alternative, and not mutually exclusive, hypothesis is that increased food intake is a homeostatic mechanism to sustain enhanced EE. Although we do not provide clear evidence to disentangle these two hypotheses, the fact remains that NAPE-PLD knock-down in the VTA confers a protective phenotype against HFD-induced body fat gain and metabolic alterations (Fig. 6). This result nicely echoes a study in humans that has identified a common haplotype of the Napepld gene in severe obesity [28]. In view of our results, one should consider that VTA NAPE-PLD deletion led to a protective effect against HFD-mediated fat mass gain and metabolic (mal) adaptations but was accompanied by enhanced reward-driven behaviors. This is important from a translational point of view as obesity is characterized by an alteration of peripheral and central eCBs and NAEs in humans [75–77]. Our current results, together with those depicting a role of NAPE-PLD in peripheral tissues [18, 36, 43], culminate with the elaboration of a framework in which organ- and region-specific homeostasis of NAPE/NAEs underline the complexity by which NAPE-PLD exerts its control onto reward-dependent behaviors, energy balance and body weight control.

In conclusion, our study provides direct evidence for a key role of NAPE-PLD in the control of reward-dependent behaviors, DA dynamics and energy metabolism. The main limitation of this study primarily lies in the lack of a clear cell type-specific identification of cellular and molecular mechanisms occurring within the heterogenous VTA. Given the complexity of NAEs action and the variety of bioactive lipids and signaling cascades associated with NAPE-PLD activity, further research and new investigatory tools will be required to fully comprehend the role of NAPE-PLD and its bioproducts in promoting anti-obesity strategies.

DATA AVAILABILITY

All the data generated have been included in the article. Datasets are available from the corresponding authors upon reasonable request.

REFERENCES

1. Morton GJ, Cummings DE, Baskin DG, Barsh GS, Schwartz MW. Central nervous system control of food intake and body weight. Nature. 2006;443:289–95.
2. Rossi MA, Stuber GD. Overlapping Brain Circuits for Homeostatic and Hedonic Feeding. Cell Metab. 2018;27:42–56.
3. de Araujo IE, Schatzker M, Small DM. Rethinking Food Reward. Annu Rev Psychol. 2020;71:139–64.
4. Berland C, Small DM, Luquet S, Gangarossa G. Dietary lipids as regulators of reward processes: multimodal integration matters. Trends Endocrinol Metab. 2021;32:693–705.
5. Mock ED, Gagestein B, van der Stelt M. Anandamide and other N-acylethanolamines: A class of signaling lipids with therapeutic opportunities. Prog Lipid Res. 2023;89:101194.
6. Hussain Z, Uyama T, Tsuboi K, Ueda N. Mammalian enzymes responsible for the biosynthesis of N -acylethanolamines. Biochim Biophys Acta. 2017;1862:1546–61.
7. Okamoto Y, Morishita J, Tsuboi K, Tonai T, Ueda N. Molecular characterization of a phospholipase D generating anandamide and its congeners. J Biol Chem. 2004;279:5298–305.
8. Ahern GP. Activation of TRPV1 by the satiety factor oleoylethanolamide. J Biol Chem. 2003;278:30429–34.
9. Fu J, Gaetani S, Oveisi F, Lo Verme J, Serrano A, Rodriguez De Fonseca F, et al. Oleylethanolamide regulates feeding and body weight through activation of the nuclear receptor PPAR-alpha. Nature. 2003;425:90–93.
10. Lo Verme J, Fu J, Astarita G, La Rana G, Russo R, Calignano A, et al. The nuclear receptor peroxisome proliferator-activated receptor-alpha mediates the anti-inflammatory actions of palmitoylethanolamide. Mol Pharm. 2005;67:15–19.
11. Cristino L, Becker T, Di Marzo V. Endocannabinoids and energy homeostasis: an update. Biofactors. 2014;40:389–97.
12. Esposito G, Capoccia E, Turco F, Palumbo I, Lu J, Steardo A, et al. Palmitoylethanolamide improves colon inflammation through an enteric glia/toll like receptor 4-dependent PPAR-α activation. Gut. 2014;63:1300–12.
13. Hansen HS, Vana V. Non-endocannabinoid N-acylethanolamines and 2-monoacylglycerols in the intestine. Br J Pharm. 2019;176:1443–54.
14. Rodriguez de Fonseca F, Navarro M, Gomez R, Escuredo L, Nava F, Fu J, et al. An anorexic lipid mediator regulated by feeding. Nature. 2001;414:209–12.
15. Terrazzino S, Berto F, Dalle Carbonare M, Fabris M, Guiotto A, et al. Stearoylethanolamide exerts anorexic effects in mice via down-regulation of liver stearoyl-coenzyme A desaturase-1 mRNA expression. FASEB J. 2004;18:1580–2.
16. DiPatrizio NV. Endocannabinoids in the Gut. Cannabis Cannabinoid Res. 2016;1:67–77.
17. Fu J, Kim J, Oveisi F, Astarita G, Piomelli D. Targeted enhancement of oleoylethanolamide production in proximal small intestine induces across-meal satiety in rats. Am J Physiol Regul Integr Comp Physiol. 2008;295:R45–50.
18. Everard A, Plovier H, Rastelli M, Van Hul M, de Wouters d'Oplinter A, Geurts L, et al. Intestinal epithelial N-acylphosphatidylethanolamine phospholipase D links dietary fat to metabolic adaptations in obesity and steatosis. Nat Commun. 2019;10:457.
19. Melis M, Pillolla G, Luchicchi A, Muntoni AL, Yasar S, Goldberg SR, et al. Endogenous Fatty Acid Ethanolamides Suppress Nicotine-Induced Activation of

Mesolimbic Dopamine Neurons through Nuclear Receptors. J Neurosci. 2008;28:13985–94.
20. Palese F, Pontis S, Realini N, Piomelli D. A protective role for N-acylphosphatidylethanolamine phospholipase D in 6-OHDA-induced neurodegeneration. Sci Rep. 2019;9:15927.
21. Tevosian M, Todorov H, Lomazzo E, Bindila L, Ueda N, Bassetti D, et al. NAPE-PLD deletion in stress-TRAPed neurons results in an anxiogenic phenotype. Transl Psychiatry. 2023;13:152.
22. Morishita J, Okamoto Y, Tsuboi K, Ueno M, Sakamoto H, Maekawa N, et al. Regional distribution and age-dependent expression of N-acylphosphatidylethanolamine-hydrolyzing phospholipase D in rat brain. J Neurochem. 2005;94:753–62.
23. Egertova M, Simon GM, Cravatt BF, Elphick MR. Localization of N-acyl phosphatidylethanolamine phospholipase D (NAPE-PLD) expression in mouse brain: A new perspective on N-acylethanolamines as neural signaling molecules. J Comp Neurol. 2008;506:604–15.
24. Leishman E, Mackie K, Luquet S, Bradshaw HB. Lipidomics profile of a NAPE-PLD KO mouse provides evidence of a broader role of this enzyme in lipid metabolism in the brain. Biochim Biophys Acta. 2016;1861:491–500.
25. Mock ED, Mustafa M, Gunduz-Cinar O, Cinar R, Petrie GN, Kantae V, et al. Discovery of a NAPE-PLD inhibitor that modulates emotional behavior in mice. Nat Chem Biol. 2020;16:667–75.
26. Muccioli GG. Endocannabinoid biosynthesis and inactivation, from simple to complex. Drug Discov Today. 2010;15:474–83.
27. Leung D, Saghatelian A, Simon GM, Cravatt BF. Inactivation of N-acyl phosphatidylethanolamine phospholipase D reveals multiple mechanisms for the biosynthesis of endocannabinoids. Biochemistry. 2006;45:4720–6.
28. Wangensteen T, Akselsen H, Holmen J, Undlien D, Retterstøl L. A common haplotype in NAPEPLD is associated with severe obesity in a Norwegian population-based cohort (the HUNT study). Obesity. 2011;19:612–7.
29. Doris JM, Millar SA, Idris I, O'Sullivan SE. Genetic polymorphisms of the endocannabinoid system in obesity and diabetes. Diabetes Obes Metab. 2019;21:382–7.
30. Sun F, Zhou J, Dai B, Qian T, Zeng J, Li X, et al. Next-generation GRAB sensors for monitoring dopaminergic activity in vivo. Nat Methods. 2020;17:1156–66.
31. Berland C, Castel J, Terrasi R, Montalban E, Foppen E, Martin C, et al. Identification of an endocannabinoid gut-brain vagal mechanism controlling food reward and energy homeostasis. Mol Psychiatry. 2022;27:2340–54.
32. Berland C, Montalban E, Perrin E, Di Miceli M, Nakamura Y, Martinat M, et al. Circulating Triglycerides Gate Dopamine-Associated Behaviors through DRD2-Expressing Neurons. Cell Metab. 2020;31:773–e11.
33. Gangarossa G, Castell L, Castro L, Tarot P, Veyrunes F, Vincent P, et al. Contrasting patterns of ERK activation in the tail of the striatum in response to aversive and rewarding signals. J Neurochem. 2019;151:204–26.
34. Raboune S, Stuart JM, Leishman E, Takacs SM, Rhodes B, Basnet A, et al. Novel endogenous N-acyl amides activate TRPV1-4 receptors, BV-2 microglia, and are regulated in brain in an acute model of inflammation. Front Cell Neurosci. 2014;8:195.
35. Liu J, Wang L, Harvey-White J, Huang BX, Kim HY, Luquet S, et al. Multiple pathways involved in the biosynthesis of anandamide. Neuropharmacology. 2008;54:1–7.
36. Geurts L, Everard A, Van Hul M, Essaghir A, Duparc T, Matamoros S, et al. Adipose tissue NAPE-PLD controls fat mass development by altering the browning process and gut microbiota. Nat Commun. 2015;6:6495.
37. Lallemand Y, Luria V, Haffner-Krausz R, Lonai P. Maternally expressed PGK-Cre transgene as a tool for early and uniform activation of the Cre site-specific recombinase. Transgenic Res. 1998;7:105–12.
38. Giusti SA, Vercelli CA, Vogl AM, Kolarz AW, Pino NS, Deussing JM, et al. Behavioral phenotyping of Nestin-Cre mice: implications for genetic mouse models of psychiatric disorders. J Psychiatr Res. 2014;55:87–95.
39. Tronche F, Kellendonk C, Kretz O, Gass P, Anlag K, Orban PC, et al. Disruption of the glucocorticoid receptor gene in the nervous system results in reduced anxiety. Nat Genet. 1999;23:99–103.
40. Declercq J, Brouwers B, Pruniau VPEG, Stijnen P, de Faudeur G, Tuand K, et al. Metabolic and Behavioural Phenotypes in Nestin-Cre Mice Are Caused by Hypothalamic Expression of Human Growth Hormone. PLoS One. 2015;10:e0135502.
41. Tellez LA, Han W, Zhang X, Ferreira TL, Perez IO, Shammah-Lagnado SJ, et al. Separate circuitries encode the hedonic and nutritional values of sugar. Nat Neurosci. 2016;19:465–70.
42. Tellez LA, Medina S, Han W, Ferreira JG, Licona-Limon P, Ren X, et al. A gut lipid messenger links excess dietary fat to dopamine deficiency. Science. 2013;341:800–2.
43. Rastelli M, Van Hul M, Terrasi R, Lefort C, Regnier M, Beiroa D, et al. Intestinal NAPE-PLD contributes to short-term regulation of food intake via gut-to-brain axis. Am J Physiol Endocrinol Metab. 2020;319:E647–E657.
44. Morales I, Berridge KC. 'Liking' and 'wanting' in eating and food reward: Brain mechanisms and clinical implications. Physiol Behav. 2020;227:113152.
45. Savell KE, Tuscher JJ, Zipperly ME, Duke CG, Phillips RA, Bauman AJ, et al. A dopamine-induced gene expression signature regulates neuronal function and cocaine response. Sci Adv. 2020;6:eaba4221.
46. Phillips RA, Tuscher JJ, Black SL, Andraka E, Fitzgerald ND, Ianov L, et al. An atlas of transcriptionally defined cell populations in the rat ventral tegmental area. Cell Rep. 2022;39:110616.
47. Brichta L, Shin W, Jackson-Lewis V, Blesa J, Yap EL, Walker Z, et al. Identification of neurodegenerative factors using translatome-regulatory network analysis. Nat Neurosci. 2015;18:1325–33.
48. Aguila J, Cheng S, Kee N, Cao M, Wang M, Deng Q, et al. Spatial RNA Sequencing Identifies Robust Markers of Vulnerable and Resistant Human Midbrain Dopamine Neurons and Their Expression in Parkinson's Disease. Front Mol Neurosci. 2021;14:699562.
49. Montalban E, Walle R, Castel J, Ansoult A, Hassouna R, Foppen E, et al. The addiction-susceptibility TaqIA/Ankyrin repeat and kinase domain containing 1 kinase (ANKK1) controls reward and metabolism through dopamine receptor type 2 (D2R)-expressing neurons. Biol Psychiatry. 2023;94:424–36.
50. Woodworth HL, Batchelor HM, Beekly BG, Bugescu R, Brown JA, Kurt G, et al. Neurotensin Receptor-1 Identifies a Subset of Ventral Tegmental Dopamine Neurons that Coordinates Energy Balance. Cell Rep. 2017;20:1881–92.
51. Fernandes MFA, Matthys D, Hryhorczuk C, Sharma S, Mogra S, Alquier T, et al. Leptin Suppresses the Rewarding Effects of Running via STAT3 Signaling in Dopamine Neurons. Cell Metab. 2015;22:741–9.
52. Medrano M-C, Hurel I, Mesguich E, Redon B, Stevens C, Georges F, et al. Exercise craving potentiates excitatory inputs to ventral tegmental area dopaminergic neurons. Addict Biol. 2021;26:e12967.
53. Muguruza C, Redon B, Fois GR, Hurel I, Scocard A, Nguyen C, et al. The motivation for exercise over palatable food is dictated by cannabinoid type-1 receptors. JCI Insight. 2019;4:e126190.
54. Dubreucq S, Durand A, Matias I, Bénard G, Richard E, Soria-Gomez E, et al. Ventral tegmental area cannabinoid type-1 receptors control voluntary exercise performance. Biol Psychiatry. 2013;73:895–903.
55. Lunerti V, Li H, Benvenuti F, Shen Q, Domi A, Soverchia L, et al. The multitarget FAAH inhibitor/D3 partial agonist ARN15381 decreases nicotine self-administration in male rats. Eur J Pharmacol. 2022;928:175088.
56. Melis M, Scheggi S, Carta G, Madeddu C, Lecca S, Luchicchi A, et al. PPARα regulates cholinergic-driven activity of midbrain dopamine neurons via a novel mechanism involving α7 nicotinic acetylcholine receptors. J Neurosci. 2013;33:6203–11.
57. Melis M, Carta S, Fattore L, Tolu S, Yasar S, Goldberg SR, et al. Peroxisome proliferator-activated receptors-alpha modulate dopamine cell activity through nicotinic receptors. Biol Psychiatry. 2010;68:256–64.
58. Hempel B, Crissman M, Pari S, Klein B, Bi G-H, Alton H, et al. PPARα and PPARγ are expressed in midbrain dopamine neurons and modulate dopamine- and cannabinoid-mediated behavior in mice. Mol Psychiatry. 2023. https://doi.org/10.1038/s41380-023-02182-0.
59. Guillaumin MCC, Viskaitis P, Bracey E, Burdakov D, Peleg-Raibstein D. Disentangling the role of NAc D1 and D2 cells in hedonic eating. Mol Psychiatry. 2023;28:3531–47.
60. Grace AA. The tonic/phasic model of dopamine system regulation and its implications for understanding alcohol and psychostimulant craving. Addiction. 2000;95:S119–128.
61. Tsai H-C, Zhang F, Adamantidis A, Stuber GD, Bonci A, de Lecea L, et al. Phasic firing in dopaminergic neurons is sufficient for behavioral conditioning. Science. 2009;324:1080–4.
62. Floresco SB, West AR, Ash B, Moore H, Grace AA. Afferent modulation of dopamine neuron firing differentially regulates tonic and phasic dopamine transmission. Nat Neurosci. 2003;6:968–73.
63. Kreitzer AC, Regehr WG. Retrograde signaling by endocannabinoids. Curr Opin Neurobiol. 2002;12:324–30.
64. Nyilas R, Dudok B, Urbán GM, Mackie K, Watanabe M, Cravatt BF, et al. Enzymatic machinery for endocannabinoid biosynthesis associated with calcium stores in glutamatergic axon terminals. J Neurosci. 2008;28:1058–63.
65. Pupe S, Wallén-Mackenzie Å. Cre-driven optogenetics in the heterogeneous genetic panorama of the VTA. Trends Neurosci. 2015;38:375–86.
66. Morales M, Margolis EB. Ventral tegmental area: cellular heterogeneity, connectivity and behaviour. Nat Rev Neurosci. 2017;18:73–85.
67. Wang H-L, Qi J, Zhang S, Wang H, Morales M. Rewarding Effects of Optical Stimulation of Ventral Tegmental Area Glutamatergic Neurons. J Neurosci. 2015;35:15948–54.
68. Root DH, Barker DJ, Estrin DJ, Miranda-Barrientos JA, Liu B, Zhang S, et al. Distinct Signaling by Ventral Tegmental Area Glutamate, GABA, and Combinatorial Glutamate-GABA Neurons in Motivated Behavior. Cell Rep. 2020;32:108094.

69. Zell V, Steinkellner T, Hollon NG, Warlow SM, Souter E, Faget L, et al. VTA Glutamate Neuron Activity Drives Positive Reinforcement Absent Dopamine Co-release. Neuron. 2020;107:864–e4.
70. O'Connor EC, Kremer Y, Lefort S, Harada M, Pascoli V, Rohner C, et al. Accumbal D1R Neurons Projecting to Lateral Hypothalamus Authorize Feeding. Neuron. 2015;88:553–64.
71. Diepenbroek C, Rijnsburger M, van Irsen AAS, Eggels L, Kisner A, Foppen E, et al. Dopamine in the nucleus accumbens shell controls systemic glucose metabolism via the lateral hypothalamus and hepatic vagal innervation in rodents. Metabolism. 2023;150:155696.
72. Boekhoudt L, Omrani A, Luijendijk MCM, Wolterink-Donselaar IG, Wijbrans EC, van der Plasse G, et al. Chemogenetic activation of dopamine neurons in the ventral tegmental area, but not substantia nigra, induces hyperactivity in rats. Eur Neuropsychopharmacol. 2016;26:1784–93.
73. Perez-Bonilla P, Santiago-Colon K, Matasovsky J, Ramirez-Virella J, Khan R, Garver H, et al. Activation of ventral tegmental area neurotensin Receptor-1 neurons promotes weight loss. Neuropharmacology. 2021;195:108639.
74. Mietlicki-Baase EG, Reiner DJ, Cone JJ, Olivos DR, McGrath LE, Zimmer DJ, et al. Amylin modulates the mesolimbic dopamine system to control energy balance. Neuropsychopharmacology. 2015;40:372–85.
75. Fanelli F, Mezzullo M, Repaci A, Belluomo I, Ibarra Gasparini D, Di Dalmazi G, et al. Profiling plasma N-Acylethanolamine levels and their ratios as a biomarker of obesity and dysmetabolism. Mol Metab. 2018;14:82–94.
76. Jumpertz R, Guijarro A, Pratley RE, Piomelli D, Krakoff J. Central and peripheral endocannabinoids and cognate acylethanolamides in humans: association with race, adiposity, and energy expenditure. J Clin Endocrinol Metab. 2011;96:787–91.
77. Mazier W, Saucisse N, Gatta-Cherifi B, Cota D. The Endocannabinoid System: Pivotal Orchestrator of Obesity and Metabolic Disease. Trends Endocrinol Metab. 2015;26:524–37.

ACKNOWLEDGEMENTS

We thank Olja Kacanski for administrative support, Isabelle Le Parco, Aurélie Djemat, Daniel Quintas, Magguy Boa, Ludovic Maingault, Angélique Dauvin and Florianne Michel for animals' care and genotyping. We thank Dr. Etienne Doumazane for clustering analyses and Dr. Sylvie Robin for the gift of Villin-Cre^{ERT2} mice. We acknowledge the technical platform Functional and Physiological Exploration platform (FPE) of the Université Paris Cité, CNRS, Unité de Biologie Fonctionnelle et Adaptative, and the animal core facility "Buffon" of the Université Paris Cité/Institut Jacques Monod.

AUTHOR CONTRIBUTIONS

Conceptualization: GG and SL; Investigation: JC, GL, OO, AE, EL, HB, KM, PDC, SL, GG; Formal Data Analysis: JC, SL, GG, HB, KM, AE; Resources: GG, SL, PDC; Funding acquisition: GG, SL, PDC; Supervision: GG and SL; Writing – original draft: GG and SL; Writing – review & editing: all authors.

FUNDING

This work was supported by the Nutricia Research Foundation (#2022-E7), *Agence Nationale de la Recherche* (ANR-21-CE14-0021-01, ANR-23-CE14-0014-02, ANR-19-CE37-0020-02), *Fondation pour la Recherche Médicale* (Équipe FRM #EQU202003010155), *Fédération pour la Recherche sur le Cerveau* and *Association France Parkinson*, *Institut universitaire de France*, the Modern Diet and Physiology Research Center (MDPRC), Université Paris Cité, US National Institutes of Health (DA047858), and CNRS. GL is supported by a China Scholarship Council (CSC) fellowship. OO is supported by an FRM fellowship. PDC is recipient of grants from FNRS (FRFS-WELBIO: WELBIO-CR-2022A-02, EOS: program no. 40007505) and La Caixa (NeuroGut). AE is research associate at FNRS and the recipient of grants from FNRS (FRFS-WELBIO: WELBIO-CR-2019S-03R, FNRS: J.0075.22).

COMPETING INTERESTS

PDC and AE are inventors on patent applications dealing with the use of specific bacteria and components in the treatment of different diseases. PDC was co-founder of The Akkermansia Company SA and Enterosys. The other authors declare no competing interests.

ADDITIONAL INFORMATION

Supplementary information The online version contains supplementary material available at https://doi.org/10.1038/s41380-024-02427-6.

Correspondence and requests for materials should be addressed to Serge Luquet or Giuseppe Gangarossa.